



Diel behavior of stable isotopes of dissolved oxygen and dissolved inorganic carbon in rivers over a range of trophic conditions, and in a mesocosm experiment

Stephen R. Parker^{a,*}, Christopher H. Gammons^b, Simon R. Poulson^c, Michael D. DeGrandpre^d, Charmaine L. Weyer^a, M. Garrett Smith^a, John N. Babcock^b, Yasuhiro Oba^c

^a Department of Chemistry and Geochemistry, Montana Tech of The University of Montana, 1300 W. Park St., Butte, MT 59701, USA

^b Dept. of Geological Engineering, Montana Tech of The University of Montana, Butte, MT 59701, USA

^c Dept. of Geological Sciences and Engineering, University of Nevada-Reno, Reno, NV 89557, USA

^d Dept. of Chemistry, The University of Montana, Missoula, MT 59812, USA

ARTICLE INFO

Article history:

Accepted 17 June 2009

Keywords:

Diel
Dissolved oxygen
Dissolved inorganic carbon
Stable isotopes
Trophic state

ABSTRACT

Rates of diel (24-h) biogeochemical processes in rivers and their effect on daily changes in the concentration of metals and metalloids have been well documented in the literature over the last 20 years. Investigations into the effects of these processes on aquatic systems and the underlying mechanisms that control the processes can significantly improve our understanding of how natural aquatic environments function and will respond to changing environmental conditions and anthropogenic impacts. Daily changes in the rates of biogeochemical processes have, more recently, been shown to influence the stable isotope composition of dissolved oxygen and dissolved inorganic carbon in natural waters. Here we present a comprehensive picture of the persistence and reproducibility of diel cycles of the ¹⁸O composition of dissolved molecular oxygen ($\delta^{18}\text{O}$ -DO) and the ¹³C composition of dissolved inorganic carbon ($\delta^{13}\text{C}$ -DIC) across five Montana, USA rivers investigated over a 4-year period. A mesocosm experiment showed the same behavior in $\delta^{18}\text{O}$ -DO and $\delta^{13}\text{C}$ -DIC as seen in riverine settings across light and dark periods.

A cross plot of $\delta^{18}\text{O}$ -DO and $\delta^{13}\text{C}$ -DIC from each stream exhibits a clockwise elliptical pattern which is attributed to the daily changes in the balance of metabolic rates as well as air–water gas exchange. The amplitude of the change in the isotope composition is shown to be directly related to the trophic state of the river and a relationship between net productivity and diel changes in $\delta^{18}\text{O}$ -DO and $\delta^{13}\text{C}$ -DIC is presented. This relationship between trophic status with $\delta^{18}\text{O}$ -DO, $\delta^{13}\text{C}$ -DIC and production emphasizes the significance of how rates of biogeochemical processes in natural systems can influence the daily changes in the composition of surface waters.

© 2009 Elsevier B.V. All rights reserved.

1. Introduction

Diel processes in flowing surface waters are regular, dynamic changes in physical and biogeochemical parameters that occur over 24-h periods and play an integral role in the health of natural water systems. Normally functioning rivers can exhibit large diel pH, O₂ and CO₂ cycles that are largely driven by aquatic plants and microbes alternately consuming or producing CO₂ depending on whether photosynthesis or respiration is the dominant process (Odum, 1956; Pogue and Anderson, 1994; Nagorski et al., 2003; Parker et al., 2005).

Many studies have detailed diel concentration fluctuations of metals and arsenic in streams (e.g., Nimick et al., 1998, 2003, 2005; Jones et al., 2004; Gammons et al., 2005a,b; Parker et al., 2007a,b and references therein). Although these studies have contributed to the knowledge

and understanding of diel processes, there is much that is not well understood. Rivers are biologically productive and physically dynamic systems that host a myriad of chemical interfaces between ambient air, the mixed water column, suspended solids, biofilm and periphyton, hyporheic ground water, and mineral substrates. There is a critical need to better understand the interrelationships between the various phases and components. Knowledge of the underlying mechanisms controlling diel concentration changes will allow us to make better predictions of how rivers and streams will react to changing conditions of eutrophication, climate change, drought, industrialization, and other variables.

Analysis of the 18:16-O composition of dissolved molecular oxygen ($\delta^{18}\text{O}$ -DO) and the 13:12-C ratio in dissolved inorganic carbon ($\delta^{13}\text{C}$ -DIC) in surface waters has shown that photosynthesis, respiration and gas exchange can influence the isotope composition of DO and DIC (Quay et al., 1993, 1995; Wassenaar and Koehler, 1999; Russ et al., 2004; Parker et al., 2005, 2007b; Tobias et al., 2007; Venkiteswaran et al., 2007, 2008). The global average $\delta^{18}\text{O}$ of atmospheric oxygen is 23.5‰ (Kroopnik and Craig, 1972) and minor fractionation during air–water

* Corresponding author. Tel.: +1 406 496 4185; fax: +1 406 496 4135.
E-mail address: sparker@mtech.edu (S.R. Parker).

Table 1

Sites sampled including dates, times, isotopes samples collected, other parameters measured, elevation, flow and location.

Site	Date(s)/time	Isotopes collected	Other parameters sampled	Stream order	Flow avg, L s ⁻¹ (range)	Elev. (m)	Location
CFR1 ^a	7/31/03, 11:30–8/1/03, 14:00	δ ¹³ C-DIC	pH, T, DO, pCO ₂ , Alk	Second	790 (711–869)	1379	46°23'N, 112° 44'W
BHR1 ^b	8/21/04, 07:00–20:00	δ ¹⁸ O-DO	pH, T, DO	Second	~5200*	1753	45°51'N, 113°05'W
BHR2 ^b	9/24/04, 17:30–9/25/04, 18:00	δ ¹⁸ O-DO, δ ¹³ C-DIC	pH, T, DO	Second	NA	1753	45°51'N, 113°05'W
DF1 ^c	8/9/05, 18:00–8/10/05, 22:00	δ ¹⁸ O-DO, δ ¹³ C-DIC	pH, T, DO	First	280 (269–337)	1683	47°03'N, 110° 40'W
MWB2 ^d	8/17/05, 16:30–8/18/05, 16:30	δ ¹⁸ O-DO, δ ¹³ C-DIC	pH, T, pCO ₂ , Alk	Second	NA	1475	46°10'N, 112° 47'W
MWB3 ^d	8/17/05, 15:30–8/18/05, 15:30	δ ¹⁸ O-DO, δ ¹³ C-DIC	pH, T, DO, pCO ₂ , Alk	Second	460 (440–490)	1470	46°10'N, 112°47'W
CFR2	7/27/06, 11:15–7/28/06, 13:15	δ ¹³ C-DIC	pH, T, DO	Second	1170† (1076–1218)	1379	46°23'N, 112° 44'W
BHRG1	8/8/06, 10:00–8/9/06, 11:00	δ ¹³ C-DIC	pH, T, DO, Alk	Second	1614† (850–1953)	1792	45°48'N, 113°18'W
SBC3	7/23/07, 10:00–7/24/07, 10:00	δ ¹⁸ O-DO, δ ¹³ C-DIC	pH, T, DO, Alk	First	406 (325–485)	1634	46°00'N, 112°36'W
BHRG2	7/31/07, 10:30–8/1/07, 10:00	δ ¹³ C-DIC	pH, T, DO, Alk	Second	2698† (2379–3030)	1792	45°48'N, 113°18'W

All times are MDT (–0600 GMT); T = temperature; DO = dissolved oxygen; pCO₂ = partial pressure wet CO₂; Alk = alkalinity; NA = not available. *Flow at BHR-2 is an estimate based on measured flow 2 weeks before this event; †Flow at CFRG and BHRG from USGS gage adjacent to sampling site.

^a Parker et al. (2007a).

^b Parker et al. (2005).

^c Nimick et al. (2007).

^d Gammons et al. (2007).

gas exchange drives aqueous DO to an equilibrium value of 24.2‰. Photosynthesis by aquatic photoautotrophs produces DO that is similar in isotopic composition to the source water (Guy et al., 1993; Telmer and Veizer, 2000) and since the δ¹⁸O-H₂O of most natural waters is lower than the δ¹⁸O of air, photosynthesis tends to lower the δ¹⁸O-DO in a river, lake or ocean water. This is particularly true in regions like Montana, USA that have meteoric water which is isotopically depleted relative to ocean water due to a cold climate and/or high continentality (Clark and Fritz, 1997; Gammons et al., 2006). Conversely, community respiration causes kinetic isotopic fractionation that increases the δ¹⁸O of residual DO in the water (Kroopnik, 1975; Guy et al., 1993). The result of these contrasting effects is that the δ¹⁸O-DO signature in a river tends to decrease to lower values during the day, and increase to higher values during the night (Parker et al., 2005; Tobias et al., 2007; Venkiteswaran et al., 2007, 2008).

Venkiteswaran et al. (2007) developed the “PoRGy” model to construct diel δ¹⁸O-DO curves using published equilibrium and kinetic isotopic enrichment factors and user-defined input data on DO concentrations and metabolic (photosynthesis, P; respiration, R) and gas exchange (G) rates. However, the model does not include the possible accrual of DO from ground water discharge into the study system. In highly productive systems, contributions of O₂ from ground water may be negligible compared to the oxygen dynamics driven by photosynthesis and respiration but this may not be the case in less productive waters. Tobias et al. (2007) showed that δ¹⁸O-DO data can be used to determine the relative and absolute rates of photosynthesis (P) and respiration (R) during a 24-h period and pointed out that R changes as a function of temperature and the metabolic state of activity. Although the model of Tobias et al. (2007) does include possible contributions of O₂ from ground water discharge, the input data needed to calibrate the model may be difficult to obtain.

Although it has received less attention in the literature, changes in the stable isotopic composition of dissolved inorganic carbon (δ¹³C-DIC) can also theoretically be used to track diel changes in metabolic rates. During photosynthesis, when CO₂ concentration is not diffusion limited, aquatic photoautotrophs utilize ¹²CO₂ as a C-source at a faster rate than ¹³CO₂ (Falkowski and Raven, 1997); consequently, the remaining DIC is isotopically enriched. Conversely, community respiration produces CO₂ that has an isotopic signature similar to that of the indigenous vegetation (Clark and Fritz, 1997). In temperate regions such as Montana, C₃ plants are the dominant species in both aquatic and terrestrial regimes with δ¹³C values in the range of –20 to –30‰ (Clark and Fritz, 1997). Thus, in the absence of competing reactions, biological processes tend to increase δ¹³C-DIC during the day, and decrease δ¹³C-DIC during the night, a pattern which is the reverse of δ¹⁸O-DO. However, because the average 24-h concentration of DIC in most natural waters is much larger than that of DO, the magnitude of

the diel change in δ¹³C-DIC induced by biological reactions is usually smaller than that of δ¹⁸O-DO. As well, a number of confounding circumstances may obscure the biological signal in δ¹³C-DIC, including air–water gas exchange, influx of DIC from high-alkalinity ground water, and precipitation or dissolution of carbonate minerals. Atmospheric CO₂ in the western USA is typically in the range of –7.5 to –8.5‰ (NOAA, 2008). Equilibrium fractionation during dissolution of CO₂(g) into water should produce CO₂(aq) with δ¹³C = –8.2 to –9.7‰, and HCO₃⁻ with δ¹³C = –1 to +3‰ (Clark and Fritz, 1997). However, because complete equilibrium is rarely attained between DIC in the various air, water, and mineral phases, the 24-h average δ¹³C-DIC of a given surface water may deviate substantially from what would be predicted based on equilibration with atmospheric CO₂. Finlay (2003) showed that in 6 streams in Northern California δ¹³C-DIC was most strongly influenced by pCO₂, not pH, Ca²⁺ or watershed area; suggesting that stream productivity and its impact on pCO₂ will be the most important determinant of stream δ¹³C-DIC.

Although previous workers have reported diel changes in either δ¹³C-DIC or δ¹⁸O-DO, there has been no study to date, other than Parker et al. (2005), that combines these two parameters across a broad range of river conditions. This paper examines the behavior of δ¹³C-DIC and δ¹⁸O-DO from five Montana rivers over a period from July 2003 to July 2007 (Table 1) and relates this behavior to the net productivity (i.e., trophic state) of the system. Three of the isotope data sets have been published previously and are included here with five new data sets to help construct a comprehensive picture of the influences of in-stream diel biogeochemical processes on the stable isotope composition of DO and DIC. The effects of high nutrient concentrations of anthropogenic origin on δ¹³C-DIC and δ¹⁸O-DO are also reported here for one field site downstream from a municipal waste water outfall. Additionally, a laboratory mesocosm experiment was performed to investigate the effects of photosynthesis and respiration on the isotopic systematics of DO and DIC under controlled conditions.

2. Field sites

Geographic locations, sampling dates, isotopes sampled and average water chemistries for each field investigation are given in Table 1 and Fig. 1. Sampling locations in the Clark Fork River watershed include one site on Silver Bow Creek (SBC3) near the city of Butte, two sites on the Mill-Willow Bypass (MWB2 and MWB3) near the town of Warm Springs, and two sites on the Clark Fork River (CFR1 and CFR2) near the city of Deer Lodge. All of these locations lie within the upper Clark Fork River National Priority Area, which is the largest EPA Superfund site by land area in the USA. The mining and smelting centers of Butte and Anaconda are situated at the headwaters of the upper Clark Fork River along Silver Bow and Warm Springs Creeks, respectively

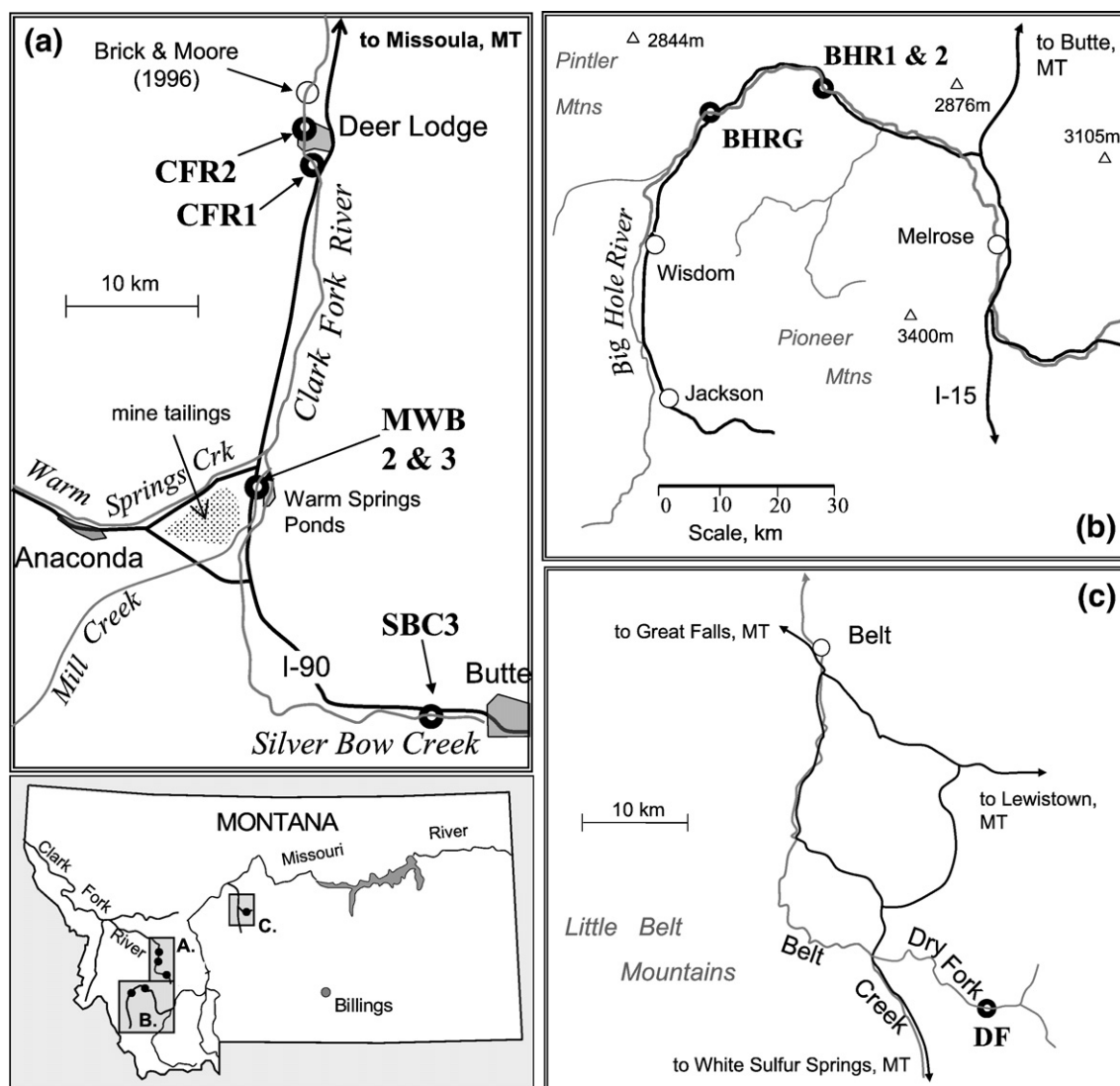


Fig. 1. Location map showing the sampling sites in the Clark Fork (a), Big Hole (b) and Belt Creek (c) watersheds. Relative locations in Montana are indicated in the lower left panel.

(Fig. 1a). Besides being negatively impaired by residual heavy metals (e.g., Moore and Luoma, 1990; Hochella et al., 2005), these waters also suffer high nutrient loads and are therefore subject to seasonal algal blooms and chronic eutrophication. This is particularly true of Silver Bow Creek at SBC3, which is located only a few km downstream of the municipal sewage treatment plant of Butte (pop. ~35,000).

The Mill-Willow Bypass (Fig. 1a) is a partially engineered second-order, meandering stream course which directs the combined flows of Mill Creek and Willow Creek around the Warm Springs Ponds Operational Unit, a large pond and wetland area used to remove Cu and other heavy metals from Silver Bow Creek; additional details can be found in Duff (2001), EPA (2005), and Gammons et al. (2007). The two sampling locations in this study at Mill-Willow Bypass are located 900 m (MWB2) and 50 m (MWB3) upstream of the confluence with the treated discharge from the Warm Springs Ponds Operational Unit. The stream distance between sites was estimated from aerial photographs to be ~1300 m.

The upper Clark Fork River (Fig. 1a) is formed from the confluence of Silver Bow Creek and Warm Springs Creek, about 1.7 km downstream from the MWB3 site described above. This section of the Clark Fork is a second-order stream with a discharge ranging from 600 to 6000 L s⁻¹, depending on the time of year. The CFR1 and CFR2 sampling sites referred to in this paper are approximately 2.8 and 1.8 km

upstream, respectively, from the site used in the 1994 diel study of Brick and Moore (1996). The CFR1 site reported here is the AS2 site of Parker et al. (2007b). The CFR2 site is adjacent to the USGS gaging station (12324200) at Deer Lodge.

Two locations were sampled on the Big Hole River, a major tributary of the upper Missouri River (Fig. 1b). The Big Hole River drains a high elevation basin of approximately 7200 km², and is free-flowing throughout its 243 km length. The river is relatively pristine and highly prized as a wild trout fishery, and the watershed is sparsely-populated with few historical impacts from mining or industrial sources (see BHRG2, Table 2). The field site used in 2005 is near the Dickie Bridge section of the middle reach of the Big Hole (see Parker et al., 2005) and two separate samplings at this site are reported here, labeled BHR1 and BHR2. The BHRG site is approximately 25 km upstream from Dickie Bridge directly adjacent to USGS stream gaging station 06024540. Two separate samplings were conducted at BHRG; named BHRG1 and 2.

Diel isotopic data were also collected on the Dry Fork of Belt Creek (DF1), a fast flowing mountain stream approximately 70 km southeast of Great Falls, MT (Fig. 1c, Table 1). This small, first-order stream has been heavily impacted by historical mining operations. Collection of isotopic samples reported in this study coincided with a field experiment which examined the effects of daily concentration changes of

Table 2
Selected physical and chemical parameters for all sites reported.

Sites	pH	Alk	T	DO, % sat.	SC	Ca	Na	K
CFR1	8.24 (7.95–8.54)	3624 (3481–3710)	18.8 (15.2–22.7)	111 (67–167)	508 (498–516)	1290 (1210–1340)	978 (957–1000)	96.4 (98–102)
BHR1	8.49 (7.71–8.90)	NA	16.6 (12.9–19.1)	112 (79.2–140)	149 (143–157)	NA	NA	NA
BHR2	8.08 (7.57–8.62)	NA	10.8 (6.9–13.6)	105 (90.3–123)	108 (106–109)	NA	NA	NA
DF1	8.19 (8.08–8.26)	1905 (1886–1926)	12.1 (9.5–15.9)	101 (96–102)	254 (250–257)	836 (765–885)	83.5 (67.0–92.8)	20.3 (18.7–21.6)
MWB2	8.35 (7.96–8.82)	2532 (2404–2667)	15.1 (11.7–18.7)	NA	630 (592–657)	1977 (1837–2123)	658 (626–685)	79.4 (72.5–85.7)
MWB3	8.38 (7.92–8.84)	2629 (2489–2750)	15.3 (11.6–20.0)	106 (69.3–153)	504 (494–521)	2096 (1960–2229)	660 (644–689)	81.9 (74.7–85.2)
CFR2	8.06 (7.73–8.42)	NA	20.3 (16.3–24.8)	105 (62.9–159)	1244 (846–1404)	NA	727 (480–878)	90.3 (73.8–100)
BHRG1	9.13 (8.44–9.38)	NA	17.8 (14.5–21.70)	88.2 (36.8–156.9)	158 (148–172)	NA	NA	NA
SBC3	7.16 (7.07–7.36)	2020 (1838–2178)	18.5 (16.0–21.3)	36.4 (6.4–89.5)	577 (554–596)	1014 (965–1068)	703 (674–770)	151 (128–164)
BHRG2	8.12 (7.55–8.71)	1365 (1199–1698)	19.0 (14.8–24.3)	82.6 (52–124)	149 (142–156)	254 (130–271)	635 (304–749)	70 (36–79)
Sites	Mg	Cl ⁻	SO ₄ ²⁻	Mn	Zn	Cu	Cd	$\delta^{18}\text{O-H}_2\text{O}$
CFR1	492 (478–509)	298 (291–313)	627 (619–637)	0.67 (0.45–0.95)	0.081 (0.037–0.12)	0.079 (0.052–0.24)	0.005 (0.004–0.006)	NA
BHR1	NA	NA	NA	NA	NA	NA	NA	-16.1 (± 0.1 , n = 13)
BHR2	NA	NA	NA	NA	NA	NA	NA	-17.0 (± 0.04 , n = 19)
DF1	346 (321–362)	5.4 (5.1–6.0)	347 (337–351)	26.7 (25.0–29.0)	7.8 (5.9–9.5)	0.057 (0.035–0.079)	0.025 (0.019–0.033)	NA
MWB2	768 (724–815)	NA	NA	1.2 (0.1–1.9)	<0.06	NA	NA	NA
MWB3	818 (774–852)	167 (75.8–209)	1823 (1537–2051)	1.33 (0.89–2.60)	0.029 (0.004–0.078)	0.036 (0.028–0.047)	NA	-16.5 (± 0.09 , n = 3)
CFR2	456 (301–510)	NA	624 (404–680)	0.39 (0.26–0.58)	0.086 (0.041–0.27)	0.17 (0.11–0.29)	<0.008	NA
BHRG1	NA	NA	NA	NA	NA	NA	NA	NA
SBC3	403 (385–423)	446 (423–482)	438 (393–468)	2.85 (1.71–3.95)	0.39 (0.07–0.83)	0.16 (0.14–0.20)	0.0011 (0.009–0.0014)	-16.9 (± 0.08 , n = 6)
BHRG2	105 (55–112)	69.2 (64.3–75.3)	20.9 (27.6–34.7)	0.27 (0.03–0.62)	<0.06	<0.047	<0.009	NA

Average value and range (parenthesis) listed for each parameter. pH = stand. units; Alk = alkalinity, $\mu\text{eq L}^{-1}$; T = temperature, °C; DO = dissolved oxygen, % sat.; SC = specific conductivity, $\mu\text{S cm}^{-1}$; all analytes are filtered solutions (0.1 or 0.2 μm), $\mu\text{mol L}^{-1}$, $\delta^{18}\text{O-H}_2\text{O}$ per mil; NA = not available.

metals (e.g., Zn, Cd) on survival of juvenile trout (Nimick et al., 2007). The streambed at DF1 was visibly devoid of significant periphyton, most likely due to the steep gradient, low trophic status and high concentrations of metals that are toxic to aquatic life (e.g., Cu, Cd, Zn; Table 2).

3. Methods

3.1. Field methods

In situ temperature, pH, DO and specific conductivity were measured at each sampling site usually hourly or every other hour with an *in situ* Troll 9000 or Hydrolab MS5 datasonde and/or a hand-held meter (WTW-340i). The instruments were calibrated according to manufacturer's specifications using standard buffers for the pH electrode and water saturated air for the DO probe. The accuracy of the DO probes was cross-checked by split analysis of selected samples using the Winkler method (Wetzel and Likens, 1991). The DO probe at MWB2 failed and consequently DO data were not recorded for that site.

A submersible autonomous moored instrument (SAMI-CO₂, DeGrandpre et al., 1995, 1999) for measuring pCO₂ was deployed at CFR1, MWB2 and MWB3. Each SAMI-CO₂ recorded pCO₂ (μatm) and temperature at 15 min intervals throughout the diel sampling. The SAMI-CO₂ instruments were calibrated prior to deployment, and precision of the wet pCO₂ determination is estimated to be $\pm 12 \mu\text{atm}$ at 1400 μatm (Baehr and DeGrandpre, 2004). Values of pCO₂ were not measured for BHR2, BHRG, CFRG and DF1 but were calculated using CO2SYS (Lewis and Wallace, 1998) with the measured pH, temperature and alkalinity. Total alkalinity of unfiltered water was measured onsite using the open-cell potentiometric titration method (Dickson et al., 2003) and Gran plot analysis (Edmond, 1970). This method was estimated to have a precision within $\pm 10 \mu\text{eq kg}^{-1}$ based on replicate titrations and an accuracy of $\pm 10 \mu\text{eq kg}^{-1}$ based on the titration of four low ionic strength sodium carbonate standards.

Samples for stable isotope analysis of ¹⁸O of dissolved oxygen ($\delta^{18}\text{O-DO}$) were collected at BHR1, BHR2, DF1, MWB2, MWB3 and SBC3. Samples were collected in septum capped, acid-washed, pre-evacuated 125 mL serum bottles containing 50 μL of saturated HgCl₂ (Wassenaar and Koehler, 1999; Parker et al., 2005). Samples were collected in the field by puncturing the septum with a syringe needle while holding under water in a well-mixed, flowing section of the stream, approximately half-way between the surface and the bottom. The bottles were allowed to fill until pressure equilibrated and the needle was removed under water. The headspace in these bottles that was created by exsolution of the dissolved gases was later sampled for isotope analysis of DO.

Filtered water samples for ¹³C-isotope analysis of dissolved inorganic carbon ($\delta^{13}\text{C-DIC}$) were collected during all sampling events listed in Table 1 using a peristaltic pump and disposable 142 mm diameter 0.1- μm cellulose-ester filter membranes (Gammons et al., 2005a) or 0.2 μm PES syringe filters (Parker et al., 2005). These samples were collected in 125 mL acid-washed glass bottles with plastic conical liners with no headspace and the DIC was precipitated in the laboratory as SrCO₃ after Usdowski et al. (1979). Samples (filtered) for $\delta^{18}\text{O-H}_2\text{O}$ determination were collected in 4 mL glass vials with plastic conical liners.

A light detector (LI-192SA, LI-COR) was used to measure photosynthetically active radiation (PAR) flux values (400–700 nm, $\mu\text{E m}^{-2} \text{s}^{-1}$) which were based on the manufacturer's calibration of the sensor. The non-photosynthetic period (dark period) for field and laboratory work was determined by a PAR signal of zero and was: 22:00 to 06:30 at BHR1; 19:00 to 07:30 at BHR2; 21:00 to 06:30 at DF1, CFR1, CFR2, BHRG, MWB2 and 3; and SBC3. Diel graphs that compare isotope patterns across multiple sites show a shaded region approximating the dark period from 21:00 to 06:30. All time references are local time (MDT, -06:00 GMT).

All samples collected in the field were stored on ice, in sealed plastic bags and returned to the laboratory immediately following the field work.

3.2. Laboratory methods

All mesocosm experiments were performed in 20 L aquarium tanks fitted with a recirculating waterfall for aeration and a 25 W full-spectrum grow light. The tank experiment used cobbles (2 to 10 cm diameter) coated with biofilm and attached periphyton collected from the Clark Fork River near the CFR1 sampling site (Fig. 1a, see Parker et al., 2007b) and placed in the tanks, covering the bottom. Tanks were filled with river water collected at the same site. Prior to experimental work the tanks were set to a 12-h lights-on and lights-off sequence for approximately 2 months to allow the biota to grow and adapt to the tank environment. No temperature control was used during this adaptation period. Water lost to evaporation was replaced with deionized water. At the time of the experiment the concentration of dissolved inorganic carbon (DIC) was adjusted to $\sim 2 \text{ meq L}^{-1}$ by the addition of NaHCO_3 in order to have sufficient DIC for sampling purposes. No further adjustments or water additions were made during experimental periods.

The experiment also used a control tank that was filled with deionized water and had no cobbles with periphyton but did have added NaHCO_3 (described above). Additionally, HgCl_2 was added to the control tank to an approximate concentration of 0.05 mM to retard biological activity. A circulating temperature controller was connected to coiled copper tubing in the experiment and control tanks. The temperature in the mesocosm and control tanks ranged between 12.5 and 13.5 °C. Samples were collected from both the experiment and control tanks for $\delta^{18}\text{O}$ -DO, $\delta^{13}\text{C}$ -DIC and $\delta^{18}\text{O}$ - H_2O as described in field methods. Diuron® ($\text{C}_9\text{H}_{10}\text{Cl}_2\text{N}_2\text{O}$; DCMU), which specifically interrupts electron transport by photosystem II, was added (0.5 mM) during the course of the mesocosm experiment to inhibit photosynthesis (see Morris and Meyer, 2007). Aerobic respiration is not inhibited by DCMU. The temperature, pH and DO were measured in each tank with remote datasondes and a hand-held meter as described in field methods.

3.3. Analytical methods

Samples for $\delta^{18}\text{O}$ - H_2O determination were analyzed after Epstein and Mayeda (1953) by the CO_2 equilibration technique, using a Micromass Aquaprep device interfaced to a dual inlet Micromass Isoprime stable isotope ratio mass spectrometer. Samples (SrCO_3) for $\delta^{13}\text{C}$ -DIC were analyzed using a Eurovector elemental analyzer interfaced to a Micromass Isoprime stable isotope ratio mass spectrometer after Harris et al. (1997). Analysis of samples for determination of $\delta^{18}\text{O}$ -DO followed the methods of Wassenaar and Koehler (1999) using a head-space equilibration technique. Isotope values are reported in units of ‰ in the usual δ notation versus VSMOW for oxygen and VPDB for carbon. Replicate analyses indicated a relative error of $\pm 0.1\%$ for $\delta^{18}\text{O}$ -DO and $\pm 0.05\%$ for $\delta^{13}\text{C}$ -DIC.

Analytical details for determination of dissolved metals at CFR1, MWB and DF1 have been previously reported (Parker et al., 2007b; Gammons et al., 2007; Nimick et al., 2007). Filtered, acidified (1% v/v HNO_3) samples at CFRG and SBC were collected using the above described peristaltic pump and filter system for metals.

Major and trace element concentrations of acid-preserved filtered samples were determined by inductively coupled plasma atomic emission spectroscopy (ICP-AES) and anions in unacidified samples by ion chromatography (IC). These data are presented here as supporting information for purposes of general characterization of the waters being sampled only and the analytical methods are not described in detail (see also Gammons et al., 2005a, 2007; Parker et al., 2007a,b). Ammonia ($\text{NH}_3 + \text{NH}_4^+$) was determined using filtered water by Hach method 8038 (Nessler) with an estimated detection limit of $4 \mu\text{mol L}^{-1}$ and an approximate precision (SD) of $\pm 1 \mu\text{mol L}^{-1}$.

4. Results and discussion

4.1. Field parameters

Average, minimum and maximum values for pH, temperature, alkalinity, specific conductivity (SC), dissolved oxygen (DO, % sat and $\mu\text{mol L}^{-1}$), and selected analytes are listed for the ten diel data sets included in this paper (Table 2). All of the streams showed significant diel changes in pH (>0.9 units) and DO ($>40\%$ change in saturation) with the exception of DF1 ($\Delta\text{pH} \approx 0.05$; $\Delta\text{DO} \approx 6\%$ sat).

4.2. Field $\delta^{18}\text{O}$ -DO diel cycles

Consistent diel patterns in $\delta^{18}\text{O}$ -DO were seen at most of the sites reported here, with 24-h changes in $\delta^{18}\text{O}$ ($\Delta\delta^{18}\text{O}$ -DO) of 7.7 to 21.6‰ (Fig. 2a). In contrast, DF1 had a very narrow range in $\delta^{18}\text{O}$ ($\Delta\delta^{18}\text{O}$ -DO = 0.6‰) and a 24-h average $\delta^{18}\text{O}$ -DO of 23.2‰, which is 1‰ below the atmospheric equilibrium value of 24.2‰ but close to the global atmospheric value of 23.5‰. At night the $\delta^{18}\text{O}$ -DO at DF1 did not increase above atmospheric equilibrium. Most sites had a minimum to maximum change in percent saturation of dissolved O_2 $>40\%$ with maxima well above 100%. Again, the exception was DF1 where DO varied over a much smaller range of 96 to 102% (256 – $276 \mu\text{mol L}^{-1}$) with an average of 101% (Table 2 and Fig. 2b). This indicates that only small contributions from photosynthesis and community respiration were present and this is consistent with the DO and $\delta^{18}\text{O}$ -DO being largely controlled by rapid re-aeration with atmospheric O_2 in this mountain stream.

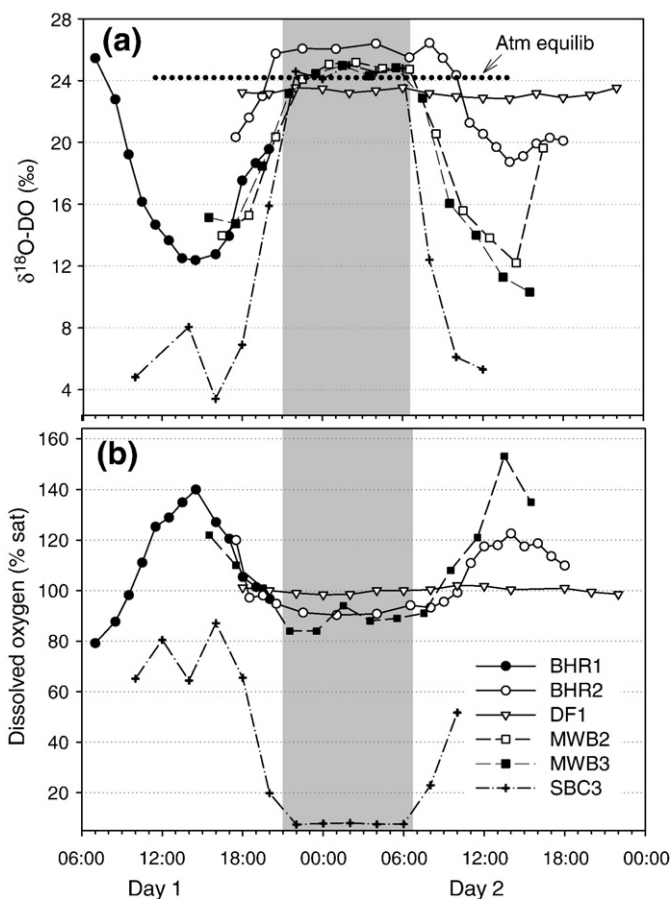


Fig. 2. Diel changes in $\delta^{18}\text{O}$ -DO (a) and % saturation of DO (b) for all sites where $\delta^{18}\text{O}$ -DO samples were collected. Shaded panels in all diel graphs approximate the night time period (PAR 0). DO data were not collected for MWB2 but should be similar to MWB3.

All the other sites (BHR1 & 2; MWB2 & 3; SBC3) reached $\delta^{18}\text{O}$ -DO levels >24.2 ‰ at night due to community respiration (Fig. 2a). All field sites were sampled during summertime base flow periods except BHR2 which was more than one month later in the season when the water temperature was lower and the day length shorter than any of the other samplings.

The two nearby sites of MWB2 and MWB3 were sampled for $\delta^{18}\text{O}$ -DO simultaneously from 17-Aug. to 18-Aug., 2005 (Fig. 3). Although the sites were separated by about 1300 m with an average water travel time of 70 min between sites, they exhibited nearly identical $\delta^{18}\text{O}$ -DO behavior. The dotted curve in Fig. 3 shows the hypothetical $\delta^{18}\text{O}$ -DO profile at MWB3 if the dissolved oxygen from MWB2 had simply advected downstream with no chemical or isotopic changes. The poor fit of the dotted curve to the field data suggests that the processes that control $\delta^{18}\text{O}$ -DO must operate on a faster time scale than the 70 min transit time between stations. The close agreement between the two field data sets also suggests that any ground water influx between sites in this wetland area had negligible effects on the isotopic composition of DO.

Silver Bow Creek at SBC3 contained unusually high levels of nutrients (NH_4^+ , NO_3^- , PO_4^{3-}), mostly due to inputs from the Butte municipal waste water treatment plant (Table 3). As a result of the high nutrient levels, the biological oxygen demand at SBC3 was unusually high and DO dropped to ~7% of saturation ($17 \mu\text{mol L}^{-1}$) at 22:00 and averaged 7.8% ($\sim 19 \mu\text{mol L}^{-1}$) for the period from 22:00 to 06:00 (Table 2 and Fig. 2b). During the same time period (22:00 to 06:00) the $\delta^{18}\text{O}$ -DO at SBC3 averaged 24.6‰ (Fig. 2a). This was very close to the atmospheric equilibrium value of 24.2‰ suggesting that aerobic respiration may have become O_2 -limited and that the low levels of DO detected in the stream during the middle of the night were due to inward diffusion from air. Using the PoRGy model, Venkiteswaran et al. (2008), showed that the night time “plateau” often found in a diel $\delta^{18}\text{O}$ -DO curve is controlled by a balance of R versus G. At low DO concentrations, oxygen availability to respiring organisms becomes transport limited resulting in an ^{18}O fractionation factor that approaches unity (Hendry et al., 2002; Hartnett et al., 2005).

During the daytime at SBC3, photosynthesis increased DO levels to a maximum of ~90% saturation ($\sim 205 \mu\text{mol L}^{-1}$) at 16:30 and at the same time $\delta^{18}\text{O}$ -DO decreased to a minimum of 3.4‰ (Fig. 4). This low value of $\delta^{18}\text{O}$ -DO indicates that photosynthetically produced O_2 comprised a larger fraction of DO than at the other sites. An afternoon period of cloudiness was reflected in a decrease in DO concentration at about 14:00 which was mirrored by an increase in $\delta^{18}\text{O}$ -DO at approximately the same time (Fig. 4). The daytime DO did not rise above 100%

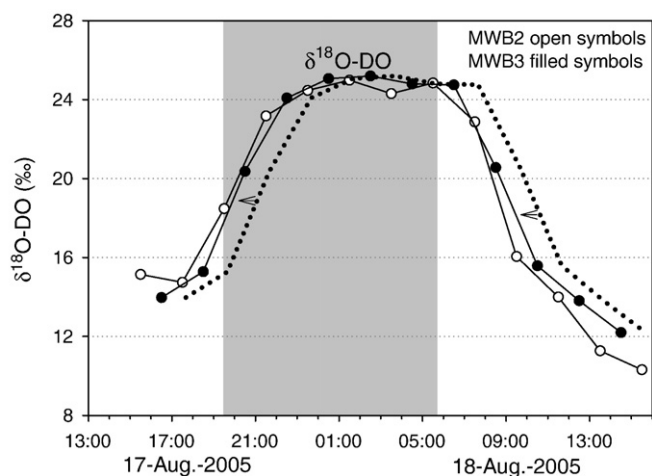


Fig. 3. Diel change in $\delta^{18}\text{O}$ -DO at MWB2 (open symbols) and MWB3 (filled symbols). Dotted line represents the approximate position of MWB2 $\delta^{18}\text{O}$ -DO trace shifted 70 minutes due to travel time between sites.

Table 3

Average, minimum and maximum concentrations of NH_4^+ , NO_3^- and PO_4^{3-} at SBC3.

Nutrient	NH_4^+	NO_3^-	PO_4^{3-}
Avg.	130	198	23.9
Min.	40.7	118	10.6
Max.	241	298	30.6

All concentrations in $\mu\text{mol L}^{-1}$ of 0.1 μm filtered solutions.

saturation at SBC3 as it did in the other studies (except DF1) despite a very thick growth of aquatic macrophytes (*Ranunculus aquatilis* and other species) choking the stream course in this reach. The main reason for the higher DO consumption rates is attributed to the input of ammonia from the Butte waste water treatment plant. Ammonia concentrations at SBC3 decreased during the daytime as nitrate levels increased (Plumb, 2009), most likely due to chemolithotrophic mediated oxidation (nitrification) of NH_4^+ to NO_3^- (Vymazal, 1995; Kowalchuk and Stephen, 2001; Galloway, 2005). The reaction proceeds with the oxidation of ammonia to nitrite most commonly by *Nitrosomonas* sp. (Eq. (1)) in freshwater. This is followed by the oxidation of nitrite to nitrate typically by *Nitrobacter* sp. (Eq. (2)).



The rate of oxidation of ammonia diminished at night at SBC3 due to low O_2 concentrations and lower temperatures (Plumb, 2009). Oxidation of reduced N compounds is assumed to have taken place with negligible fractionation of O_2 isotopes (Mayer et al., 2001). Consequently, the low $\delta^{18}\text{O}$ -DO measured at SBC3 during the daytime was most likely due to the photosynthetic production of isotopically light DO that had the same $\delta^{18}\text{O}$ of water in Silver Bow Creek ($-16.9\% \pm 0.08$, $n=6$).

4.3. Field DIC and $\delta^{13}\text{C}$ -DIC diel cycles

Aqueous DIC and CO_2 were calculated or measured (see methods) for CFR1, MWB2 and 3, SBC3, BHRG2 and DF1. Diel cycles in the concentration of DIC and CO_2 were observed for CFR1, MWB2 and 3, SBC3 and BHRG2 (Fig. 5) but, at DF1, the DIC and CO_2 did not change significantly over the diel period. The approximate concentration of CO_2 at atmospheric equilibrium (calculated at 12°C) is shown (Fig. 5b) and indicates that at MWB2 and 3 and BHRG2 the dissolved CO_2 concentration dropped below atmospheric equilibrium during the day and became oversaturated at night. At CFR1, SBC3, and DF1, CO_2 was above atmospheric equilibrium during the whole sampling period. Typically, both DIC and CO_2 decrease in concentration during the daytime as photosynthesis becomes the dominant metabolic process and then increase during the night due to community respiration.

The $\delta^{13}\text{C}$ -DIC value of the river waters increased during the day and decreased at night, and therefore showed the inverse temporal pattern to $\delta^{18}\text{O}$ -DO (Fig. 6a). The $\delta^{13}\text{C}$ -DIC cycles also showed greater variability in amplitude and average value across all sites compared to $\delta^{18}\text{O}$ -DO. The DF1 site showed a small (0.9‰) $\delta^{13}\text{C}$ -DIC change compared to 1.60 to 4.45‰ at the other sites except CFR1 which also had a 0.9‰ change in $\delta^{13}\text{C}$ -DIC. However, the CFR1 site had a diel range of DO from 67 to 167% of saturation (172 to $387 \mu\text{mol L}^{-1}$) with an average of 111% ($272 \mu\text{mol L}^{-1}$) (Table 2) indicating that there was substantial biological productivity occurring at CFR1. In contrast at DF1 the diel range of DO was only from 96 to 102% of saturation (256 – $276 \mu\text{mol L}^{-1}$) and no diel change in $\delta^{18}\text{O}$ -DO was measured. The average alkalinity at CFR1 was ~2-fold higher than DF1 (Table 2). The average pH at CFR1 and DF1 were 8.24 and 8.19, respectively. This means that the alkalinity was principally bicarbonate and the pool of DIC was larger at CFR1 than at DF1. Consequently, a 0.9‰ overall

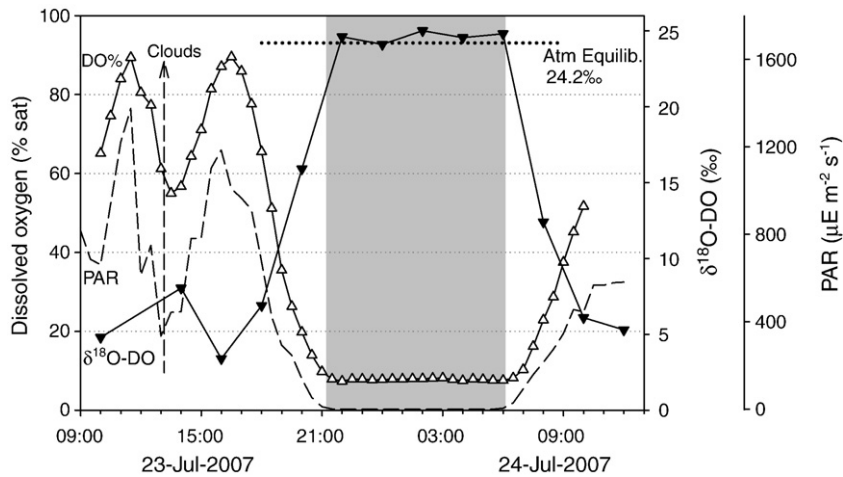


Fig. 4. Diel change in $\delta^{18}\text{O}$ -DO and % saturation of DO at SBC3. PAR and atmospheric/water isotopic (^{18}O) equilibrium of 24.2‰ are shown for reference.

change in $\delta^{13}\text{C}$ -DIC corresponds to significantly more ^{12}C and ^{13}C being added and removed from the DIC pool at CFR1 than at DF1. The fact that the average $\delta^{13}\text{C}$ -DIC values at DF1 were higher than in the other streams is likely related to low productivity since in the absence of isotopically light CO_2 from respiration the $\delta^{13}\text{C}$ -DIC can move closer to equilibrium with atmospheric CO_2 ($\delta^{13}\text{C}$ -DIC = -1 to $+3\%$ at equilibrium). The higher $\delta^{13}\text{C}$ -DIC at DF1 could be due in part to a greater percentage of DIC sourced from dissolution of limestone. The watershed upstream of DF1 contains bedrock exposures of the Mississippian Madison Limestone which has been shown elsewhere to yield $\delta^{13}\text{C}$ -

carbonate values of $3.1 \pm 1.2\%$ (Plummer et al., 1990). Additionally, Finlay (2003) showed that the $\delta^{13}\text{C}$ -DIC in shaded, mountain streams (i.e., DF1) was higher than that of broad valley rivers that received more sunlight, had warmer waters and consequently a more productive algal community.

At the paired sites of MWB2 and 3 the diel behavior of $\delta^{13}\text{C}$ -DIC was nearly identical and also in-phase as was observed with the $\delta^{18}\text{O}$ -DO at these sites (Fig. 3). This suggests that the processes modifying the isotopic composition of DIC operated on a time scale significantly shorter than the 70 min water travel time between these two sites.

The $\delta^{13}\text{C}$ -DIC at SBC3 showed a diel change of 4.5‰ which is greater than the average diel change of 1.9‰ (± 0.62) at the other sites (Fig. 6a). This large diel swing in $\delta^{13}\text{C}$ -DIC is consistent with the large change

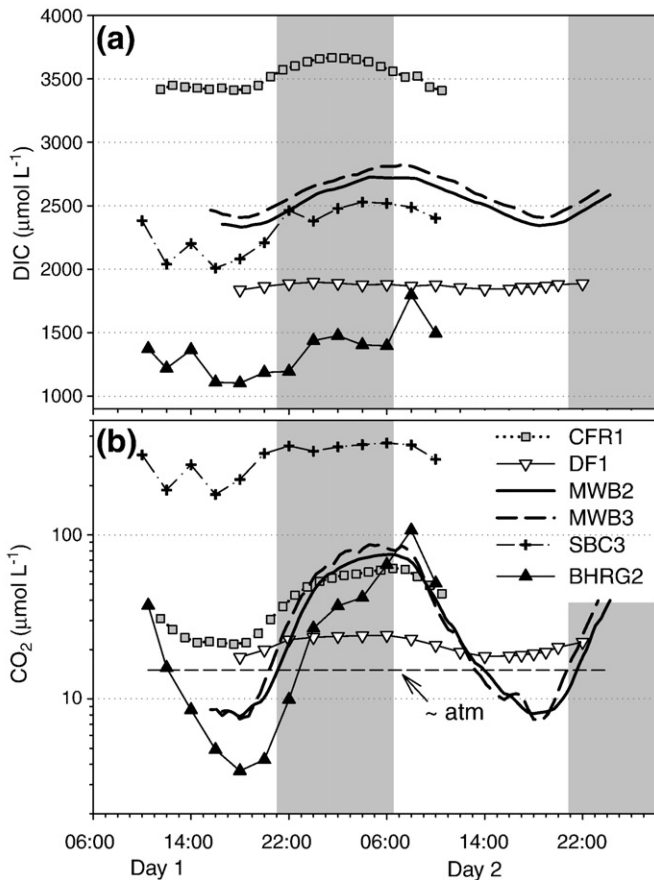


Fig. 5. Concentrations of DIC (a) and CO_2 (b) ($\mu\text{mol L}^{-1}$) over all reported sites. The approximate atmospheric CO_2 saturation is shown on graph (dashed line).

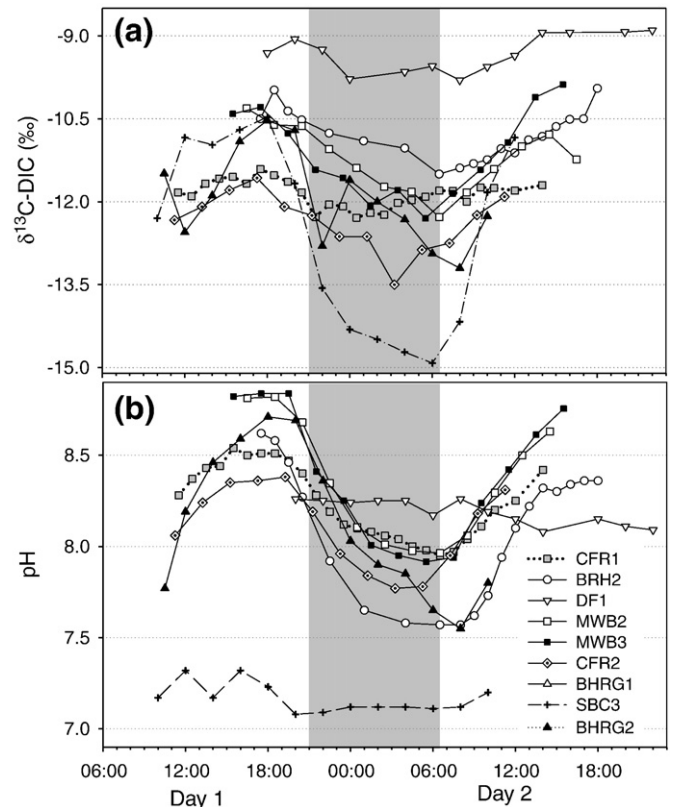
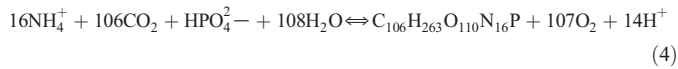
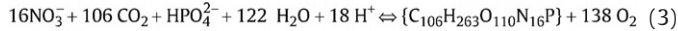


Fig. 6. Diel changes in $\delta^{13}\text{C}$ -DIC (a) and pH (b) over all reported sites.

in $\delta^{18}\text{O}$ -DO described above (Section 4.2) and is a direct result of the hyper-eutrophic environment present at SBC3. The afternoon increase in $\delta^{18}\text{O}$ -DO observed at SBC3 which correlated with the corresponding decrease in PAR due to a cloudy period (Fig. 4) was not seen in the $\delta^{13}\text{C}$ -DIC data since the average concentration of DIC was ~25-times larger than that of the DO. Assuming a metabolic relationship of ~1:1 between CO_2 and O_2 , and ignoring side reactions such as air-gas exchange or mineral dissolution/precipitation, the absolute change in the molal concentration of O_2 over the diel period should have been ~25-times larger than for total DIC.

Aquatic photosynthetic communities assimilate NH_4^+ , NO_3^- and PO_4^{3-} as well as CO_2 during the production of biomass (Eqs. (3) and (4)); Stumm and Morgan, 1996).

← Respiration Photosynthesis →



These reactions are part of the primary fixation of inorganic to organic carbon. Despite the abnormally high inorganic N and P levels present at SBC3, which created hyper-eutrophic conditions, the C-isotope fractionation associated with Eqs. (3) and (4) will not change. However, the rates of these reactions were accelerated which led to the large diel ranges in $\delta^{18}\text{O}$ -DO and $\delta^{13}\text{C}$ -DIC measured at SBC3.

4.4. Mesocosm experiment

An aquarium tank mesocosm experiment was performed to demonstrate the effects of photosynthesis, respiration and gas exchange

on the isotopic composition of DIC and DO in a controlled laboratory environment. The pH during the first two days in the experiment tank showed a regular change that was influenced by a net consumption of CO_2 due to photosynthesis during light periods and production of CO_2 when respiration alone was the determining biochemical process during the lights-off periods (Fig. 7a). In the control tank the pH showed a small regular change that had the inverse temporal pattern to that of the experiment tank which is most likely due to the small changes in temperature. To verify that the pH variation in the control tank was due to the temperature change the pH was modeled using CO2SYS, alkalinity and estimated $p\text{CO}_2$ calculated from Henry's Law which produced pH fluctuations of similar magnitude and the same direction as observed in the control tank (not shown). The temperature increase during the dark period was apparently due to an over-compensation of the temperature controller to the heat input from the grow lights during the lights-on period (Fig. 7b).

The $\delta^{18}\text{O}$ -DO values in the experiment tank decreased for the first two days during the lights-on period due to greater amounts of isotopically light O_2 being produced by photosynthesis and increased at night as respiration preferentially removing the lighter ^{16}O versus ^{18}O (Fig. 7c). The DO concentration in the experiment tank showed the inverse temporal pattern to that of the $\delta^{18}\text{O}$ -DO; increasing during the lights-on period and decreasing during the dark period. Water in the experiment tank had $\delta^{18}\text{O}$ of -12.1% (± 0.01 , $n = 2$), and was the source of oxygen for the photosynthetic production of O_2 .

The $\delta^{13}\text{C}$ -DIC values during this same time period (first two days) showed the inverse temporal pattern to the $\delta^{18}\text{O}$ -DO, becoming isotopically enriched during the day as photosynthesis preferentially removed lighter $^{12}\text{CO}_2$ and becoming depleted at night as respiration returned isotopically light CO_2 to the water column (Fig. 7c). The $\delta^{13}\text{C}$ -DIC and $\delta^{18}\text{O}$ -DO in the control tank showed no changes in response to the lights-on and -off periods, nor to the small fluctuations

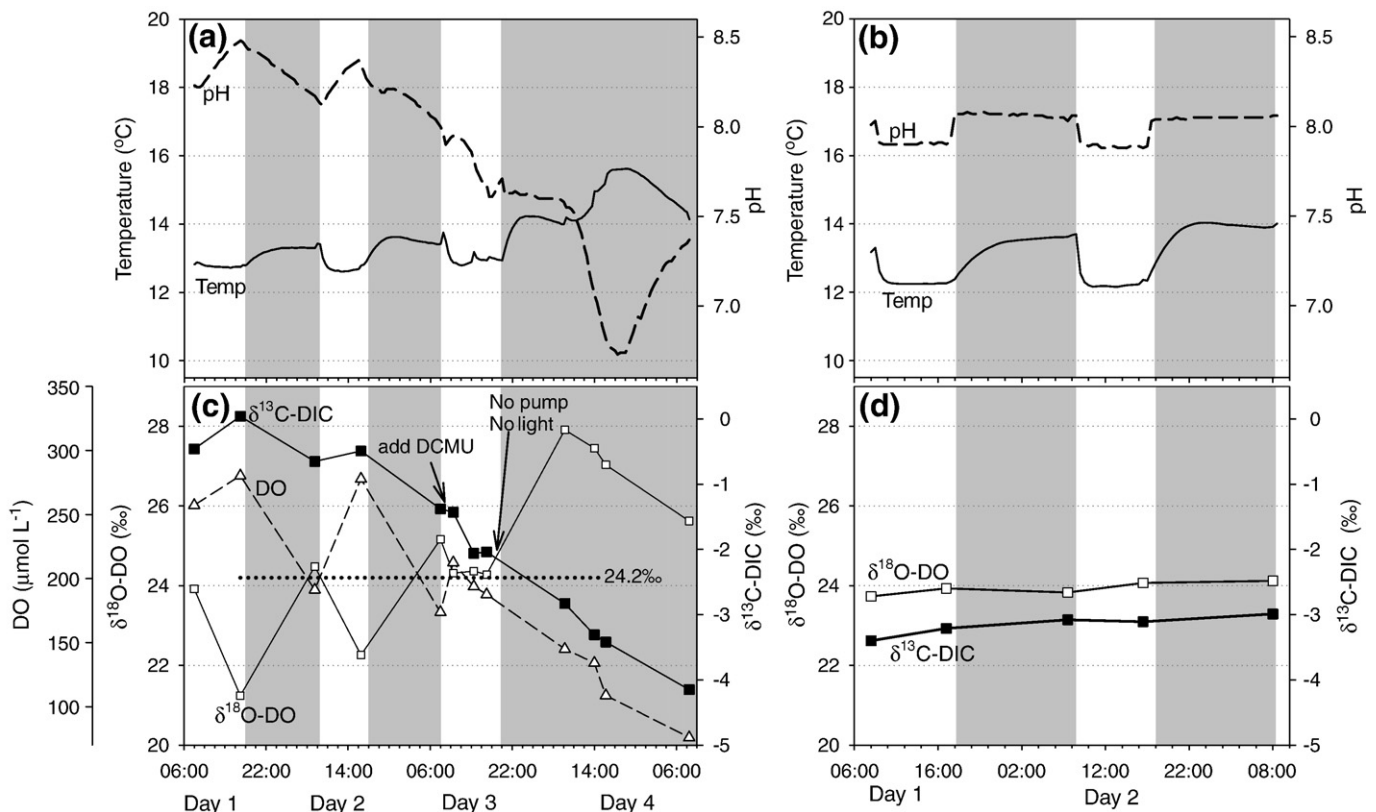


Fig. 7. Mesocosm experiment results showing: the pH and temperature in the experiment (a) and control (b) tanks; and the DO, $\delta^{18}\text{O}$ -DO and $\delta^{13}\text{C}$ -DIC in the experiment (c) and control (d) tank. The addition of DCMU is shown (c) as well as the atmospheric/water isotopic (^{18}O) equilibrium of 24.2‰ (dotted line).

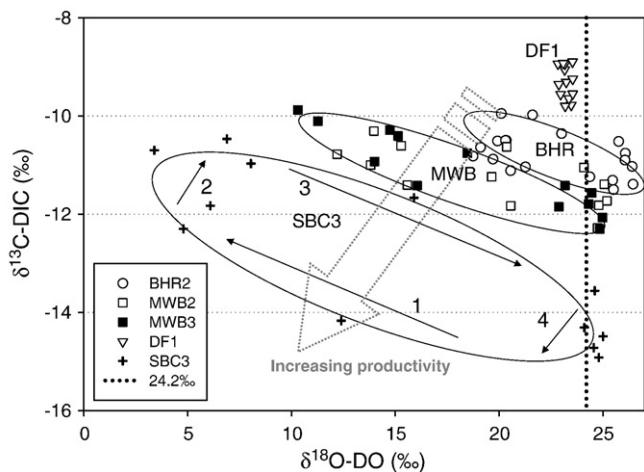


Fig. 8. The relationship of $\delta^{18}\text{O-DO}$ and $\delta^{13}\text{C-DIC}$ is shown for data from four streams. Ellipses have been drawn to approximate the diel pattern followed by the isotope compositions. Arrows in the SBC3 ellipse show the diel direction (clockwise) of the change in isotope composition and numbers (1, 2, 3, 4) refer to discussion in the text. The general increasing direction of the diel change in net productivity (ΔP_{net}) is shown by the large arrow (see Table 5).

in temperature and pH (Fig. 7d). At 09:00 on day three DCMU was added to the experiment tank to inhibit photosynthesis. The $\delta^{18}\text{O-DO}$ did not decrease after addition of DCMU as it had during the previous two lights-on periods (Fig. 7c). The $\delta^{13}\text{C-DIC}$ began decreasing immediately after the DCMU addition and did so throughout the remainder of the experiment indicating that photosynthetic consumption of CO_2 ceased with the DCMU application while respiration continued to add isotopically light CO_2 . At 16:00 the aeration/circulation pump and lights were turned off and the isotopic composition of DO responded immediately with the $\delta^{18}\text{O-DO}$ increasing (Fig. 7c) to a maximum of 27.9‰ by 08:00 the next morning. This maximum is well above the atmospheric equilibrium value of 24.2‰ and the DO at this time was 56% of saturation ($144 \mu\text{mol L}^{-1}$). After 08:00 the DO and $\delta^{18}\text{O-DO}$ decreased until the end of the experiment (Fig. 7c). Since no light was available for photosynthesis and respiration was continuing to contribute isotopically light CO_2 as shown by the decrease in $\delta^{13}\text{C-DIC}$, the decline in $\delta^{18}\text{O-DO}$ after 08:00 is attributed to a rate of infiltration of atmospheric O_2 that caused the isotopic composition of $\delta^{18}\text{O-DO}$ to decrease as the DO saturation continued to decline. This decrease in $\delta^{18}\text{O-DO}$ demonstrates the importance of gas exchange to the isotope composition of DO, especially at low DO concentrations.

The results discussed above from DF1 are consistent with the control tank mesocosm experiment in which little change was observed in $\delta^{13}\text{C-DIC}$ and $\delta^{18}\text{O-DO}$ over two lights-on and -off cycles (Fig. 7d). In the absence of active metabolic processes the isotope compositions do not change.

4.5. Relationship between $\delta^{13}\text{C-DIC}$ and $\delta^{18}\text{O-DO}$

Parker et al. (2005) described an elliptical diel pattern between $\delta^{13}\text{C-DIC}$ and $\delta^{18}\text{O-DO}$ at BHR2, and attributed this relationship to the balance of changing metabolic rates and gas exchange for both DIC and O_2 over a 24-h period. Fig. 8 reproduces the data from Parker et al. (2005) along with 4 other data sets (this study). The combined results illustrate that elliptical diel paths in $\delta^{13}\text{C-DIC}$ and $\delta^{18}\text{O-DO}$ appear to be a common feature of rivers, and furthermore show that the amplitude of the ellipse and its deviation from atmospheric equilibrium isotopic values increases with increasing trophic state. The elliptical patterns can be better understood by examining the net productivity (P_{net} ; $\mu\text{mol O}_2 \text{ L}^{-1} \text{ h}^{-1}$) at each of these sites. P_{net} was calculated for each time step in a given diel data set based on the measured rate

of change in $[\text{O}_2]$ and the gas exchange rate (Eq. (5)); for details see Parker et al., 2005).

$$P_{\text{net}} = P_{\text{O}_2} - R_{\text{O}_2} = \frac{\Delta[\text{O}_2]}{\Delta t} - k_{\text{O}_2} \cdot ([\text{O}_2]_s - [\text{O}_2]_w) - A_{\text{O}_2} \quad (5)$$

$\Delta[\text{O}_2]/\Delta t$ is the measured change in $[\text{O}_2]$ between sampling times ($\mu\text{mol L}^{-1} \text{ time}^{-1}$); k_{O_2} is the first-order gas-exchange rate constant (time^{-1}) and can be determined from a plot of $\Delta[\text{O}_2]/\Delta t$ vs. $([\text{O}_2]_s - [\text{O}_2]_w)$ for night time data (see Parker et al., 2005); $[\text{O}_2]_s$ is the calculated molar concentration at saturation; $[\text{O}_2]_w$ the measured molar concentration in the stream; P_{O_2} is the rate of production of O_2 by photosynthesis ($\mu\text{mol L}^{-1} \text{ time}^{-1}$); R_{O_2} is the rate of consumption of O_2 by respiration ($\mu\text{mol L}^{-1} \text{ time}^{-1}$); and A_{O_2} is the accrual rate of O_2 from ground water ($\mu\text{mol L}^{-1} \text{ time}^{-1}$). P_{net} was calculated in this way for SBC3, BHR2, MWB3 and DF1 since these sites had a complete set of DO as well as $\delta^{18}\text{O-DO}$ and $\delta^{13}\text{C-DIC}$ data. Ground water contributions of O_2 were not included in the calculation of P_{net} for these sites for various reasons. The channel of Silver Bow Creek (including SBC3) in Butte, MT has been reconstructed and has little or no ground water inputs based on synoptic flow and SC measurements. The sampling site at Dickie Bridge (BHR1 and 2) was selected based on a lack of ground water inputs such that accrual of O_2 from external sources was not a factor. The MWB3 site was in a wetland area and an unknown quantity of ground water did enter the stream in the study reach. For the purposes of estimating P_{net} the O_2 accrual rate at MWB3 was assumed to be relatively constant and small compared to the changes influenced by metabolic processes in this highly productive stream as indicated by a large diel O_2 change (Table 2, Fig. 2b) as well as the fact that the diel $\delta^{18}\text{O-DO}$ and $\delta^{13}\text{C-DIC}$ cycles were in-phase at both sites (MWB2 & 3; discussed above). As stated earlier, at DF1 there was little evidence of metabolic activity. A $\sim 15\%$ diel change in flow was observed at DF1 (data not shown) which suggests that ground water flow and evapotranspiration were affecting stream flow. However, since the oxygen concentration did not change in relation to the change in flow it is assumed that the accrual of O_2 from ground water was negligible at this site (Table 2, Fig. 2b).

Calculating P_{net} based on Eq. (5) indicates that SBC3 has the largest overall minimum to maximum change [$\Delta P_{\text{net}} = P_{\text{net}}(\text{max}) - P_{\text{net}}(\text{min})$] in productivity followed by MWB3, BHR2 and DF1, respectively (Table 4). This agrees with the hierarchy of the changes reflected in the plot of $\delta^{13}\text{C-DIC}$ versus $\delta^{18}\text{O-DO}$ (Fig. 8); the larger the range in both $\delta^{13}\text{C-DIC}$ and $\delta^{18}\text{O-DO}$ ($\Delta\delta^{18}\text{O-DO}$ and $\Delta\delta^{13}\text{C-DIC}$), the larger the range in ΔP_{net} (Table 4).

The direction of change over a 24-h period around each ellipse is clockwise, as shown by the arrows in Fig. 8 (SBC3 curve), and the overall pathway can be divided into 4 time periods. During period 1 (dawn to noon, 07:00 to 12:00), the $\delta^{18}\text{O-DO}$ decreased rapidly whereas $\delta^{13}\text{C-DIC}$ increased slowly. The rapid decrease in $\delta^{18}\text{O-DO}$ was caused by the re-oxygenation of the severely O_2 -depleted water in the morning through aquatic photosynthesis. The increase in $\delta^{13}\text{C-DIC}$ during this time period is explained by preferential uptake of isotopically light $^{12}\text{CO}_2$ during photosynthesis, possibly combined with evasive loss of CO_2 to the air. Loss of CO_2 to the vapor phase would have left the

Table 4

The calculated minimum to maximum net productivity (ΔP_{net}), overall change in $\delta^{18}\text{O-DO}$ and $\delta^{13}\text{C-DIC}$ at SBC3, MWB3, BHR2 and DF1.

Site	ΔP_{net}	$\Delta\delta^{18}\text{O-DO}$	$\Delta\delta^{13}\text{C-DIC}$
SBC3	255 (−7.1 to 248)	21.6 (3.4 to 25.0)	4.5 (−12.6 to −10.3)
MWB3	133 (−43.7 to 89.6)	14.7 (10.3 to 25.0)	2.4 (−12.3 to −9.9)
BHR2	51.0 (−6.0 to 44.5)	7.7 (18.7 to 26.4)	1.6 (−11.5 to −9.9)
DF1	18.2 (−8.5 to 9.7)	0.7 (22.8 to 23.5)	0.9 (−9.8 to −8.9)

Overall or diel change shown plus range (parenthesis); $\Delta P_{\text{net}} = [P_{\text{net}}(\text{max}) - P_{\text{net}}(\text{min})]$ $\mu\text{mol O}_2 \text{ L}^{-1} \text{ h}^{-1}$; $\Delta\delta^{18}\text{O-DO}$ and $\Delta\delta^{13}\text{C-DIC}$ in ‰ VSMOW and VPDB, respectively.

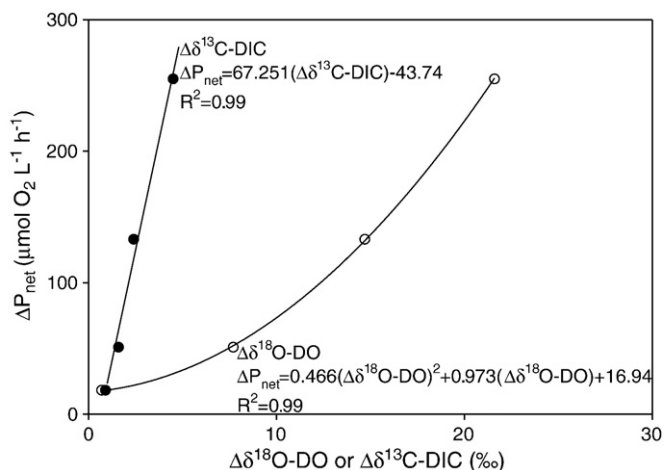


Fig. 9. The correlation between ΔP_{net} and the diel change in $\delta^{18}\text{O-DO}$ and $\delta^{13}\text{C-DIC}$ ($\Delta\delta^{18}\text{O-DO}$ and $\Delta\delta^{13}\text{C-DIC}$) at SBC3, MWB3, BHR2 and DF1. Best linear fit ($\Delta\delta^{13}\text{C-DIC}$), polynomial fit ($\Delta\delta^{18}\text{O-DO}$), equations and correlation coefficients are shown for each plot.

residual dissolved CO_2 slightly enriched in ^{13}C , due to a combination of diffusion and equilibrium processes, although the combined effect is expected to be much less than that accompanying photosynthesis. The rapid change in $\delta^{18}\text{O-DO}$ versus $\delta^{13}\text{C-DIC}$ is due to the larger concentration of DIC relative to DO. During time period 2 (mid-afternoon, 12:00 to 16:00), the $\delta^{18}\text{O-DO}$ showed little variation and attained its minimum value for the diel cycle, whereas $\delta^{13}\text{C-DIC}$ continued to increase. Early in period 2 O_2 is becoming supersaturated and since O_2 gas exchange is rapid, the slowdown in the change in $\delta^{18}\text{O-DO}$ most likely reflects a balance between continued O_2 production by photosynthesis, efflux of isotopically lighter O_2 to the atmosphere and consumption of isotopically light O_2 by respiration. During time period 3 (late afternoon to dusk, 16:00 to 20:00), the rate of photosynthesis was dwindling, while respiration rates were close to their 24-h peak, due to the warm water temperatures. This resulted in a rapid increase in $\delta^{18}\text{O-DO}$ (due to biological oxygen consumption) and a decrease in $\delta^{13}\text{C-DIC}$ (due to respiration). During time period 4 (night, 20:00 to 7:00), respiration continued in the absence of photosynthesis, resulting in a continual decrease in $\delta^{13}\text{C-DIC}$. Because DO concentrations reached extremely low levels at SBC3 ($<1 \text{ mg L}^{-1}$), respiration was likely DO-limited. Such conditions could explain the lack of any additional fractionation of $\delta^{18}\text{O-DO}$ during the night, since all available O_2 would have been utilized by respiring organisms regardless of its isotopic composition (Wassenaar and Hendry, 2007).

Fig. 9 plots relationships between the calculated values for ΔP_{net} and the observed values of $\Delta\delta^{18}\text{O-DO}$ ($R^2 = 0.94$, linear Eq. (6a); or $R^2 = 0.99$ 2nd order polynomial Eq. (6b)) and $\Delta\delta^{13}\text{C-DIC}$ ($R^2 = 0.99$, Eq. (7)) for the field sites discussed in this paper. The polynomial produces a better fit for the relationship between ΔP_{net} and $\Delta\delta^{18}\text{O-DO}$. The tendency for $\Delta\delta^{18}\text{O-DO}$ to level off at high values of ΔP_{net} is most likely due to the increasingly rapid exchange of O_2 across the air–water interface in highly productive rivers when DO concentrations are far from equilibrium with air-saturated values. In contrast, because CO_2 is much less abundant than O_2 in air, DIC concentrations are less influenced by air–water gas exchange. In the absence of competing processes (such as diurnal changes in alkalinity due to groundwater inputs), the linear relationship between ΔP_{net} and $\Delta\delta^{13}\text{C-DIC}$ (Fig. 9) is a result of in-stream biological processes.

The empirically-derived mathematical regressions in Fig. 9 could theoretically be used to estimate net productivity in other rivers based on the diel changes in the values of $\delta^{18}\text{O-DO}$ (Eq. (6b)) and $\delta^{13}\text{C-DIC}$ (Eq. (7)), or vice versa. Additionally, the overall relationship between

$\Delta\delta^{18}\text{O-DO}$ and $\Delta\delta^{13}\text{C-DIC}$ can be derived from a combination of Eqs. (6b) and (7) (Eq. (8)).

$$\Delta P_{\text{net}} = 11.36(\Delta\delta^{18}\text{O-DO}) - 12.643 \quad (6a)$$

$$\Delta P_{\text{net}} = 0.466(\Delta\delta^{18}\text{O-DO})^2 + 0.973(\Delta\delta^{18}\text{O-DO}) + 16.94 \quad (6b)$$

$$\Delta P_{\text{net}} = 67.251(\Delta\delta^{13}\text{C-DIC}) - 43.74 \quad (7)$$

$$(\Delta\delta^{13}\text{C-DIC}) = 6.93 \cdot 10^{-3}(\Delta\delta^{18}\text{O-DO})^2 + 1.45 \cdot 10^{-2}(\Delta\delta^{18}\text{O-DO}) + 0.902 \quad (8)$$

5. Conclusions: comparison of field and mesocosm results

The *in situ* stream results when viewed in relation to the mesocosm experiments reported here demonstrate that naturally occurring diel cycles in $\delta^{13}\text{C-DIC}$ and $\delta^{18}\text{O-DO}$ can be simulated using stream benthic materials and an artificial day/night cycle (Fig. 7). The mesocosm isotope composition changes were produced at nearly constant temperature which minimizes the effects of the changing solubility of dissolved gases. Additionally, in the mesocosm the absence of a flowing stream system and ground water influx eliminates the possibility that diel changes in $\delta^{13}\text{C-DIC}$ and $\delta^{18}\text{O-DO}$ are produced by the transport of new chemical species into the sampling site.

For the field sites reported here the $\delta^{18}\text{O-DO}$ showed the same behavior demonstrated during the first two lights-on and -off periods in the mesocosm; showing decreasing values during the day and increasing at night at all sites with the exception of DF1. The DF1 site was visibly devoid of attached periphyton and in absence of an impact by photosynthesis and respiration the ^{18}O -isotope composition was mainly controlled by turbulent mixing with atmospheric O_2 . These results from DF1 are consistent with the results of the mesocosm control tank. At SBC3 the $\delta^{18}\text{O-DO}$ decreased to daytime levels (Fig. 2a) well below that of the other sites due to the influence of abnormally high levels of nutrients increasing biotic productivity coupled with a smaller than normal DO concentration as a result of O_2 consumption by nitrification. The $\delta^{18}\text{O-DO}$ at night at SBC3 did not continue to increase since respiration became O_2 -limited. Furthermore, the diel DO cycle observed at SBC3 is not indicative of the true level of productivity since ammonia oxidation is consuming O_2 during the day, yet the large diel change in $\delta^{18}\text{O-DO}$ still reflects the effects of the high levels of photosynthesis and respiration.

The $\delta^{13}\text{C-DIC}$ at all field sites also displayed similar diel behavior to that simulated in the mesocosm experiment; becoming isotopically enriched during the day and depleted at night. The hierarchy of the range in net productivity (ΔP_{net}) agrees with the ranges in the diel change in $\delta^{13}\text{C-DIC}$ and $\delta^{18}\text{O-DO}$ observed at SBC3, MWB3, BHR2 and DF1 (Table 4, Fig. 9). Additionally, the $\Delta\delta^{18}\text{O-DO}$ and $\Delta\delta^{13}\text{C-DIC}$ can be used to estimate the overall productivity (ΔP_{net}) of the aquatic system (Eqs. (6b) and (7)). This confirms the strong influence of the changes in the metabolic rates on isotopic composition of DO and DIC.

Diel changes in the physical and chemical composition of rivers can have a critical impact on the concentrations of a broad spectrum of chemical species being carried in dissolved and suspended forms. This work emphasizes that rates of normal in-stream processes (respiration, photosynthesis, gas exchange, ground water contributions etc.) are significantly influencing not only the concentrations of DO and DIC, but are also producing substantial changes in the stable isotope composition of these compounds that are far from atmospheric equilibrium. Further work is needed to explore the detailed quantitative relationships between $\delta^{13}\text{C-DIC}$ and $\delta^{18}\text{O-DO}$ and the response of the isotope compositions to changing physical, chemical and biological conditions in both mesocosm and natural environments. Additionally, this approach of simultaneously monitoring changes in $\delta^{13}\text{C-DIC}$ and

$\delta^{18}\text{O}$ -DO may be valuable for monitoring processes acting on ground water systems along a flow path.

Acknowledgements

D. Nimick, A. Skerda, T. Grant, D. Snyder, B. Plumb, R. Hart, J. Lynch, S. Cullison, M. Seidel, and C. Beatty provided invaluable technical and field assistance. H. Langer, D. Smith and R. B. McClesky provided significant analytical assistance. This manuscript was greatly improved by comments from L. Stillings and two anonymous reviewers. Most of the work summarized in this paper was funded by EPA-EPSCoR grant to C. Gammons, NSF grant EAR-0337460 to M. DeGrandpre, NSF EAR-0739054 and USGS-Water-Resources Research Program grants to S. Parker. S. Poulson was funded by NSF EAR-0738912.

References

- Baehr, M.M., DeGrandpre, M.D., 2004. *In situ* pCO_2 and O_2 measurements in a lake during turnover and stratification: observations and modeling. *Limnol. Oceanogr.* 49, 330–340.
- Brick, C.M., Moore, J.N., 1996. Diel variation of trace metals in the upper Clark Fork River. *Montana. Environ. Sci. Technol.* 30, 1953–1960.
- Clark, I.D., Fritz, P., 1997. Environmental isotopes in hydrogeology. Lewis Pub, NY.
- DeGrandpre, M.D., Hammar, T.R., Smith, S.P., Sayles, F.L., 1995. A submersible autonomous sensor for spectrophotometric pH measurements of natural waters. *Limnol. Oceanogr.* 40, 969–975.
- DeGrandpre, M.D., Hammar, T.R., Smith, S.P., Sayles, F.L., 1999. Calibration-free optical chemical sensors. *Anal. Chem.* 71, 1152–1159.
- Dickson, A.G., Afghan, J.D., Anderson, G.C., 2003. Reference materials for oceanic CO_2 analysis: a method for the certification of total alkalinity. *Marine Chem.* 80, 185–197.
- Duff, B.C., 2001. Arsenic treatability study utilizing aeration and iron adsorption-coprecipitation at the Warm Springs Ponds. MS thesis, Montana Tech, Butte, Montana.
- Edmond, J.M., 1970. High precision determination of titration of alkalinity and total carbon dioxide content of sea water by potentiometric titration. *Deep-Sea Res.* 17, 737–750.
- EPA 2005. Second five-year review report for Silver Bow Creek/Butte Area Superfund Site, September 2005. <ftp://ftp.epa.gov/r8/silverbow/SilverBowCreek5YrRvw.pdf>, section 4.1, Warm Springs Ponds Operable Unit.
- Epstein, S., Mayeda, T., 1953. Variation of O^{18} content of waters from natural sources. *Geochim. Cosmochim. Acta* 4, 213–224.
- Falkowski, P.G., Raven, J.A., 1997. Aquatic Photosynthesis. Blackwell Sciences, Malden, Mass.
- Finlay, J.C., 2003. Controls of streamwater dissolved inorganic carbon dynamics in a forested watershed. *Biogeochem* 62, 231–252.
- Galloway, J.N., 2005. The Global Nitrogen Cycle. In: Schlesinger, W.H. (Ed.), *Biogeochemistry. Treatise on Geochemistry*, Vol. 8. Elsevier, Amsterdam.
- Gammons, C.H., Nimick, D.A., Parker, S.R., Cleasby, T.E., McClesky, R.B., 2005a. Diel behavior of iron and other heavy metals in a mountain stream with acidic to neutral pH: Fisher Creek, MT USA. *Geochim. Cosmochim. Acta* 69 (10), 2505–2516.
- Gammons, C.H., Wood, S.A., Nimick, D.A., 2005b. Diel behavior of rare earth elements in a mountain stream with acidic to neutral pH. *Geochim. Cosmochim. Acta* 69 (15), 3747–3758.
- Gammons, C.H., Poulson, S.R., Pellicori, D.A., Reed, P.J., Roesler, A.J., Petrescu, E.M., 2006. The hydrogen and oxygen isotopic composition of precipitation, evaporated mine water, and river water in Montana USA. *J. Hydrology* 328, 319–330.
- Gammons, C.H., Grant, T.M., Nimick, D.A., Parker, S.R., DeGrandpre, M.D., 2007. Diel changes in water chemistry in an arsenic-rich stream and treatment-pond system. *Sci. Total Environ.* 384, 433–451.
- Guy, R.D., Fogel, M.L., Berry, J.A., 1993. Photosynthetic fractionation of the stable isotopes of oxygen and carbon. *Plant Physiol.* 101, 37–47.
- Harris, D., Porter, L.K., Paul, E.A., 1997. Continuous flow isotope ratio mass spectrometry of carbon dioxide trapped as strontium carbonate. *Comm. Soil Sci. Plant Analysis* 28, 747–757.
- Hartnett, H., Devol, A., Brandes, J., Chang, B., 2005. Oxygen isotope fractionation in marine sediments during respiration. *Geochim. Cosmochim. Acta* 69 (Suppl. 1), A579.
- Hendry, M.J., Wassenaar, L.I., Birkham, T.K., 2002. Microbial respiration and diffusive transport of O-2, O-16(2), and (OO)-O-18-O-16 in unsaturated soils: a mesocosm experiment. *Geochim. Cosmochim. Acta* 66 (19), 3367–3374.
- Hochella Jr., M.F., Moore, J.N., Putnis, C.V., Putnis, A., Kasama, T., Eberl, D.D., 2005. Direct observation of heavy metal–mineral association from the Clark Fork River Superfund Complex: implications for metal transport and bioavailability. *Geochim. Cosmochim. Acta* 69 (7), 1651–1663.
- Jones, C.A., Nimick, D.A., McClesky, B., 2004. Relative effect of temperature and pH on diel cycling of dissolved trace elements in Prickly Pear Creek, Montana. *Water Air Soil Pollut.* 153, 95–113.
- Kowalchuk, G.A., Stephen, J.R., 2001. Ammonia-oxidizing bacteria: a model for molecular microbial ecology. *Annu. Rev. Microbiol.* 55, 485–529.
- Kroopnik, P.M., Craig, H.C., 1972. Atmospheric oxygen: isotopic composition and solubility fractionation. *Science* 175, 54.
- Kroopnik, P.M., 1975. Respiration, photosynthesis and oxygen isotope fractionation in oceanic surface water. *Limnol. Oceanogr.* 20, 988.
- Lewis E., Wallace D.W.R., 1998. Program developed for CO_2 system calculations. ORNL/CDIAC-105. Carbon Dioxide Information Analysis Center, Oak Ridge National Laboratory, U.S. Department of Energy, Oak Ridge, Tennessee; <http://cdiac.ornl.gov/oceans/co2rprt.html>.
- Mayer, B., Bollwerk, S.M., Mansfield, T., Hutter, B., Veizer, J., 2001. The oxygen isotope composition of nitrate generated by nitrification in acid forest floors. *Geochim. Cosmochim. Acta* 65 (16), 2743–2756.
- Moore, J.N., Luoma, S.N., 1990. Hazardous wastes from large-scale metal extraction. *Environ. Sci. Technol.* 24, 1279–1285.
- Morris, J.M., Meyer, J.S., 2007. Photosynthetically mediated Zn removal from the water column in High Ore Creek, Montana. *Water Air Soil Pollut.* 179, 391–395.
- Nagorski, S.A., Moore, J.N., McKinnon, T.E., Smith, D.B., 2003. Scale-dependent temporal variations in stream water geochemistry. *Environ. Sci. Technol.* 37, 859–864.
- Nimick, D.A., Moore, J.N., Dalby, C.E., Savka, M.W., 1998. The fate of geothermal arsenic in the Madison and Missouri Rivers. *Montana and Wyoming. Water Resour. Res.* 34, 3051–3067.
- Nimick, D.A., Gammons, C.H., Cleasby, T.E., Madison, J.P., Skaar, D., Brick, C.M., 2003. Diel cycles in dissolved metal concentrations in streams – occurrence and possible causes. *Water Resour. Res.* 39, 1247.
- Nimick, D.A., Cleasby, T.E., McClesky, R.B., 2005. Seasonality of diel cycles of dissolved trace metal concentrations in a Rocky Mountain Stream. *Environ. Geol.* 47, 603–614.
- Nimick, D.A., Harper, D.D., Farag, A.M., Cleasby, T.E., MacConnell, E., Skaar, D., 2007. Influence of in-stream diel concentration cycles of dissolved trace metals on acute toxicity to one-year-old cutthroat trout (*Oncorhynchus Clarki Lewisii*). *Environ. Toxicol. Chem.* 26 (12), 2667–2678.
- NOAA 2008. Climate monitoring and diagnostics laboratory, carbon cycle greenhouse gases: <http://www.cmdl.noaa.gov/ccgg/iadv/>.
- Odum, H.T., 1956. Primary production in flowing waters. *Limnol. Oceanogr.* 1, 102–117.
- Parker, S.R., Poulson, S.R., Gammons, C.H., DeGrandpre, M.D., 2005. Biogeochemical controls on diel cycling of stable isotopes of dissolved oxygen and dissolved inorganic carbon in the Big Hole River Montana. *Environ. Sci. Technol.* 30, 7134–7140.
- Parker, S.R., Gammons, C.H., Jones, C.A., Nimick, D.A., 2007a. Role of hydrous iron oxide formation in attenuation and diel cycling of dissolved trace metals in a stream affected by acid rock drainage. *Water. Air Soil Pollut.* 181, 247–263.
- Parker, S.R., Gammons, C.H., Poulson, S.R., DeGrandpre, M.D., 2007b. Diel variations in stream chemistry and isotopic composition of dissolved inorganic carbon; upper Clark Fork River, Montana USA. *App. Geochem.* 22, 1329–1343.
- Plumb B., 2009. Geochemistry of nutrients in Silver Bow Creek, Butte, Montana. M.S. Thesis, Montana Tech, Butte, MT, USA.
- Plummer, L.N., Busby, J.F., Lee, R.W., Hanshaw, B.B., 1990. Geochemical modeling of the Madison aquifer in parts of Montana Wyoming and South Dakota. *Water Res. Res.* 26 (9), 1981–2014.
- Pogue T.R., Anderson C.W., 1994. Processes controlling dissolved oxygen and pH in the Upper Willamette River Basin. *U.S. Geol. Surv. Water-Resources Investigations Report* 95-4205.
- Quay, P.D., Emerson, S., Wilbur, D.O., Stump, C., 1993. The $\delta^{18}\text{O}$ of dissolved O_2 in the surface waters of the subarctic Pacific: a tracer of biological productivity. *J. Geophys. Res.* 98, 8447–8458.
- Quay, P.D., Wilbur, D.O., Richey, J.E., Devol, A.H., 1995. The $^{18}\text{O}:^{16}\text{O}$ of dissolved oxygen in rivers and lakes in the Amazon Basin: determining the ratio of respiration to photosynthesis rates in freshwaters. *Limnol. Oceanogr.* 40, 718–729.
- Russ, M.E., Ostrom, N.E., Gandhi, H., Ostrom, P.H., 2004. Temporal and spatial variations in R:P ratios in Lake Superior, an oligotrophic freshwater environment. *J. Geophys. Res.* 109, C10S1.
- Stumm, W., Morgan, J.J., 1996. *Aquatic Chemistry*. John Wiley & Sons Inc, NY.
- Telmer, K., Veizer, J., 2000. Isotopic constraints on the transpiration, evaporation, energy and GPP budgets of a large boreal water-shed: Ottawa River basin, Canada. *Glob. Biogeochem. Cycles* 14, 149–166.
- Tobias, C.R., Bohlke, J.K., Harvey, J.W., 2007. The oxygen-18 isotope approach for measuring aquatic metabolism in high-productivity waters. *Limnol. Oceanogr.* 52 (4), 1439–1453.
- Uzdowski, E., Hoefs, J., Menschel, G., 1979. Relationship between ^{13}C and ^{18}O fractionation and changes in major element composition in a recent calcite-depositing spring – a model of chemical variations with inorganic CaCO_3 precipitation. *Earth Planet. Sci. Lett.* 42, 267–276.
- Venkiteswaran, J.J., Wassenaar, L.I., Schiff, S.L., 2007. Dynamics of dissolved oxygen isotopic ratios: a transient model to quantify primary production, community respiration, and air–water exchange in aquatic ecosystems. *Oecologia* 153 (2), 385–398.
- Venkiteswaran, J.J., Schiff, S.L., Wassenaar, L.I., 2008. Aquatic metabolism and ecosystem health assessment using dissolved O_2 stable isotope diel curves. *Ecol. Appl.* 18 (4), 965–982.
- Vymazal, J., 1995. *Algae and element cycling in Wetlands*. Lewis Pub, Boca Raton, FL, USA.
- Wassenaar, L.I., Koehler, G., 1999. An on-line technique for the determination of the delta O-18 and delta O-17 of gaseous and dissolved oxygen. *Anal. Chem.* 71, 4965–4968.
- Wassenaar, L.I., Hendry, M.J., 2007. Dynamics of stable isotope composition of gaseous and dissolved oxygen. *J. Ground Water* 45 (4), 447–460. doi:10.1111/j.1745-6684.2007.00328.x.
- Wetzel, R.G., Likens, G.E., 1991. *Limnological Analysis*, 2nd ed. Springer-Verlag, NY, USA.